Journal of Advances in Computer Research
Quarterly ISSN: 2008-6148
Sari Branch, Islamic Azad University, Sari, I.R.Iran
(Vol. 4, No. 2, May 2013), Pages: 25-39
www.jacr.iausari.ac.ir

Image Denoising based on Visual Patterns

Amir Ali Tahmouresi✉, Saeid Saryazdi
Department of electrical engineering, Shahid bahonar University, Kerman ,Iran
aatahmouresi@gmail.com; Saryazdi@mail.uk.ac.ir

Received: 2012/06/25; Accepted: 2013/02/04

Abstract

Among abundant image denoising methods proposed so far, the use of patch based algorithms have attracted a lot of attention from image processing community. Although these methods are very powerful in presentation of high quality results, the impact of human visual system (HVS) is ignored in sole of them. In this paper the human visual geometry is used in preparation of a new method for image denoising. Several image quality assessment (IQA) criteria, based on HVS, are used to confirm superiority of the proposed method in comparison with other state-of-the-art methods. In addition to denoising quality, the proposed method is fast as a result of dimensionality reduction.

Keywords: *Human visual system, Image denoising, Non-local means, Visual patterns*

1. Introduction

NOISE is added to digital images as an inevitable fact in result of electronic devices used for image acquisition. This noise is annoying for observer and should be mitigated. Image denoising methods have considered several aspects of image so far. For example regularization of neighborhoods [1, 2] is one of the easiest solutions for the problem of noise. This method takes advantage of weighted averaging over a neighborhood around the pixel of interest. A similar model for regularization of image is image smoothing based on partial differential equations (PDE) [3]. Regarding the regularization of image as a differential problem, an isotropic Gaussian kernel is the simplest answer, provided that the noisy image is free of sharp edges. Since natural images do not follow this limitation, an anisotropic kernel proposed by Perona and Malik has more satisfactory results. The method called “total variation reduction” which is based on PDE,smooths the image until two constrains are met [4]. First, the average of denoised and noisy image should be the same, and second, the variance of the difference of denoised and noisy image should be equal to the variance of noise. Another efficient tool for image denoising is transformation. Well-known transforms like wavelet, represent image as a spars matrix. It means that the most energy of image is limited to few coefficients, and by elimination or mitigation of other insignificant coefficients, image is regularized and noise is reduced [5].

Recently Buades et al. proposed a new method which can be classified as a neighborhood filter [6]. In this method, comparison of pixels is based on the similarity of their surrounding blocks. In addition to desirable properties like high quality results, non-local means (NLM) suffers from some disadvantages. These difficulties are listed

as: high computational complexity [7], residual artifacts in homogenous parts of image [8], and Remaining noise near high contrasted edges [9].

Initially the use of Karhunen Loeve Transform (KLT) was proposed by J. Orchard *et al.* in order to improve the performance of NLM.KLT is an optimal transform form the mathematical point of view. The authors suggested the use of singular value decomposition (SVD) to efficiently ignore unrelated patches from weighting process [10]. Tasdizen evolved their idea by means of Principal Component Analysis (PCA) to reduce the dimensionality of patterns space [11]. He used PCA to obtain most important patterns of image using a matrix made out of some blocks of image.

Due to the fact that, NLM is an effective image denoising method and KLT can greatly improve the efficiency and speed of it, this combination becomes a powerful method in reducing image noises while maintaining image details. In the other hand, besides the effectiveness of KLT, it is not optimized based on Human Visual System (HVS). HVS is an important issue that is not considered yet in image denoising methods, because a denoised image must be acceptable visually.

In this paper, first of all, a geometric system based on HVS is reviewed, and then a modified version of it is employed to construct a semi-transform, which contrary to KLT takes the properties of human eye into account. Afterwards, this transformation is used in construction of NLM method to obtain high quality denoised images in addition to complexity reduction of denoising process. The simulation results show that the proposed method is successful in improvement of denoising quality of NLM method from human point of view.

The rest of the paper is organized as follows. In Section 2 NLM filter as a powerful neighborhood regularizer is reviewed. In Section 3, the procedure of finding most important patterns in image and its significance for image denoising is explained. Section 4 is devoted to construction of visual patterns and explanation of their importance in HVS. Proposed method is presented in Section 5. In Section 6 some IQA measures based on HVS are used to compare quality of results of proposed method with other state-of-the-art image denoising algorithms. Finally the paper is concluded in Section 7.

2. Neighborhood Filters

Conventionally, a noisy image is regarded as addition of white Gaussian noise to the original image:

$$v(i) = u(i) + n(i) \tag{1}$$

Where $u(i)$,$v(i)$and $n(i)$are the values of the original image, noisy image and Gaussian white noise in the position i, respectively.

One of the most important extensions of image denoising methods is neighborhood filtering. In this method, pixels of a neighborhood$W_i$in noisy image contribute in a weighted averaging.

$$\hat{u}(i) = \sum_{j \in W_i} \frac{\omega(i,j)v(j)}{\sum_{j \in W_i} \omega(i,j)} \tag{2}$$

Where $\omega(i,j)$are weights computed based on some relations between two pixels which are compared.

Gaussian filter as the easiest image regularizer only uses spatial distances to compute weights [12].

$$\omega(i,j) = e^{-\frac{\|i-j\|^2}{h^2}} \quad (3)$$

In Eq. 3, $h$stands for filtering parameter. When it is large, image gets smoother as a result of large weights. An ordinary Gaussian filter leads to an image with smoothed and shifted edges.

It is wise to employ another characteristic of pixels, beside spatial distance, to obtain better results. This solution first was suggested by Smith and Brady [1], and then confirmed by Tomasi and Manduchi [2]. In SUSAN or Bilateral filter, distance between gray value of two pixels and the spatial distance are computed simultaneously in order to weight computation.

$$\omega(i,j) = e^{-\frac{\|i-j\|^2}{h_d^2}} e^{-\frac{\|v(i)-v(j)\|^2}{h_r^2}} \quad (4)$$

Two major disadvantage of this method are elimination of details and production of some speckle like artifacts.

It is obvious that, comparison of two groups of pixels is more robust than comparison of two single pixels. It conjures up to mind the relative frequency definition where bigger sample space leads to better results. If one assumesthese groups of pixels as some blocks of image, it could be seen thatexploiting of block similarity is more robust than the similarity of single pixels. The other evidence for the preference of blocks over pixels is redundant similar blocks in a natural image.

Consequently, Buades et al. masterminded non-local means filter [13]. In this filter, blocks of image are compared instead of comparison of single pixels. This method is robust enough to ignore spatial distances form weighting process.

$$\omega(i,j) = e^{-\frac{\|b_i-b_j\|_{2,a}^2}{2Bh^2}} \quad (5)$$

In Eq. 5$b_i$is a block centered on pixel$i$, $B$is number of pixels in the block, when$\|b_i - b_j\|_{2,a}$shows Euclidean distance and $a$is standard deviation of a Gaussian kernel which is multiplied element wise by the difference of two blocks.

Although using blocks improves the denoising quality, it imposes excessive computational complexity to the algorithm. Additionally residual noise in homogenous parts and high contrasted edges of denoised image are other main drawbacks of NLM method. For further study, a review of improvements on non-local means algorithm is available in [14].

3. Patterns Space

A complete dictionary of important patterns exists in any image, which can greatly simplify and improve the performance of block based image processing algorithms. The procedure of making this dictionary is as follows.

For each pixel of an image, a column wise vector is constructed by means of the pixels of surrounding block, and then by putting vectors next to each other, a matrix$M$is performed. Orchard et al. propose to compute the SVD of M, to remove unrelated blocks from weighting process [10]. SVD can statically represent Min several

subspaces. The importance of the subspaces is defined by their corresponding singular values. Thus, weights of NLM are computed in first sub space, and unrelated blocks are pruned from weight computation in next subspace. In this way, in addition to simplification of weight computation, the quality of results is improved thanks to reduction of the impact of unrelated blocks on denoising quality.

Likewise, another way to improve the performance of NLM is dimension reduction. In this method first covariance of matrix $M$is computed.

$$\Sigma_x = \frac{1}{|\Omega|}\sum_{k=1}^{|\Omega|}(m_i - \bar{m})(m_i - \bar{m})^T \quad (6)$$

Where$m_i$is the ith column of M, $\bar{m}$ is their average and$|\Omega|$shows their number. Next, the covariance matrix is used for eigenvalue decomposition (EVD).

$$\Sigma_x = Q\Lambda Q^{-1} \quad (7)$$

EVD leads to the eigenvalue matrix$\Lambda$when the columns of$Q$are eigenvectors which play the role of orthonormal unit vectors for patterns space. Now every single block of image can be identically defined in this space.

In [11] Tasdizen showed that by calculation of weights in a space spanned by fewer unit vectors, denoising process will be faster than conventional NLM. In his proposition, difference of two blocks is multiplied element-wise by the most important patterns of image (instead of the Gaussian kernel in Eq. 5) in order to obtain its projection along the unit vectors. These projections are then used for weight calculation. He showed, not only reduction of dimensions leads to lower computational complexity, but also, the quality of results is often more desirable. For example, to denoise Lena noisy image, results obtained from a space with 6 dimensions have lower error than those in a full 49 dimension space.

There is another related work presented in [15]. Authors of this article proposed to replace the Gaussian kernel in the weighting formula of NLM bysome shaped kernels, and the SURE measure [9, 16] is computed for each denoised image, simultaneously. Finally each single pixel of the resulted image is taken from the denoised image that provides the lowest value of SURE in its position. In other words, this method, which is called NLM-SAP, denoises image in different dimensions one by one, then uses SURE to define the best dimension for each pixel.

Taking all into account, in block based image denoising methods, there have been no attention to HVS, and needs of observer are ignored. In the next section we reviewa previous work which some suitable patters for HVS are presented in. By means of these visual patterns, denoising process aims to denoise image regarding human eye and presentation of favorable results for a normal person.

4. Visual Patterns

In order to study HVS, it is essential to construct a visual geometry. For example, details and high frequency patterns in an image are not observable for someone who is too far from screen. Further, these details cannot be shown in a screen with few numbers of pixels. Accordingly, screen size, number of its pixels and distance between observer and screen are important in human visual geometry. In this paper, some patterns are used to improve the NLM denoising algorithm in order to produce desirable results for human. Thus, the size of patterns should be designed based on human visual

geometry. Viewing geometry proposed by Chen and Bovik [17] satisfies the desire for a suitable model (Figure 1).

Assuming one is looking to an image with$L \times L$pixels showed on an$O \times O\ cm$screen, his sight angle corresponding to a$T \times T$pixels block of image isθ°.

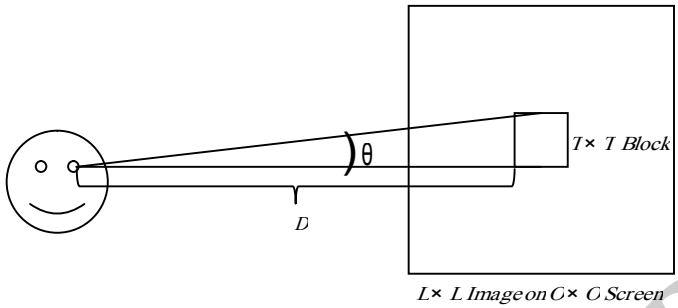

Figure 1. Average accuracy of 6 methods of decision tree

$$\theta = 180tan^{-1}\left(\frac{OT}{LD}\right) \quad (8)$$

The metrics used in [17] were suitable for many years ago. In this paper, they are revised considering a typical laptop screen. When someone is looking to a natural image or video with size$L = 512$pixels, showed on a part of a laptop screen with size$O = 11.5\ cm$, his distance from screen is fairly$D = 80\ cm$

Human eye can see 1-10 cycles of gray level value change per one degree of sight angle. The most perceivable range is 3-6 c/deg [18]. Hence, visual patterns should be small enough to only one observable edge in human visual geometry can be placed in them. Whereas, more edges in patterns, makes them complex and a small number of patterns cannot describe all possible patterns. Thus, in order to put only one edge in a pattern, based on Eq. 8, visual patterns can be of size3×3. These metrics result to$\theta \approx 0.15$which is corresponding to less than a cycle in a pattern. Proposed visual patterns are showed in Figure 2. These patterns are classified to four groups based on their gradient's angle. The rest of patterns can be obtained by their multiplication by (-1).

$$\begin{pmatrix} 1 & 1 & 1 \\ -1 & -1 & -1 \\ -1 & -1 & -1 \end{pmatrix} \quad \begin{pmatrix} 1 & 1 & 1 \\ 1 & 1 & 1 \\ -1 & -1 & -1 \end{pmatrix} \quad \text{Group } -90^{\circ}$$

$$\begin{pmatrix} -1 & 1 & 1 \\ -1 & -1 & 1 \\ -1 & -1 & -1 \end{pmatrix} \quad \begin{pmatrix} 1 & 1 & 1 \\ -1 & 1 & 1 \\ -1 & -1 & 1 \end{pmatrix} \quad \text{Group } -45^{\circ}$$

$$\begin{pmatrix} -1 & -1 & 1 \\ -1 & -1 & 1 \\ -1 & -1 & 1 \end{pmatrix} \quad \begin{pmatrix} -1 & 1 & 1 \\ -1 & 1 & 1 \\ -1 & 1 & 1 \end{pmatrix} \quad \text{Group } 0^{\circ}$$

$$\begin{pmatrix} -1 & -1 & -1 \\ -1 & -1 & 1 \\ -1 & 1 & 1 \end{pmatrix} \quad \begin{pmatrix} -1 & -1 & 1 \\ -1 & 1 & 1 \\ 1 & 1 & 1 \end{pmatrix} \quad \text{Group } 45^{\circ}$$

Figure 2. Visual patterns

5. Proposed Method

As it is aforementioned, two previous works done by Tasdizen and Orchard focused on use of KLT to make some patterns for improvement of NLM.In the previous section some patterns better matching HVS were reviewed.In the proposed method, these patterns are used in a de-noising process based on NLM method to improve its performance in favor of HVS.

Three strategies could be considered for a visual pattern image denoising. First strategy consists of finding most repeated patterns in an image, and then using them as unit vectors for patterns space, and computing weights in this space. The second one does like the first strategy but in a limited neighborhood,W_i.In the third strategy, the best counterpart pattern for central block of$W_i$is selected and used then to compare the central block with others in neighborhoodW_i. Because of a lower computational complexity, easier implementation and higher performance due to locally choosing of patterns, we opt forthird strategy.

In the proposed method, visual patterns are assigned to blocks of the input image according to their gradient's angle. Then, these visual patterns contribute in computation of weights. The flowchart of the proposed method is depicted in Figure 3.

As this figure shows,for all3×3blocks of input image, the most appropriate pattern from patterns showed in Figure 2 should be chosen. To this, the gradient's angle of blocks is computed.

$$\Delta_x b = mean\big(b(x+2, y{:}\, y+2)\big) - mean(b(x, y{:}\, y+2)) \tag{9}$$

$$\Delta_y b = mean\big(b(x{:}\, x+2, y+2)\big) - mean(b(x{:}\, x+2, y)) \tag{10}$$

$$\measuredangle \Delta b = tan^{-1}\left(\frac{\Delta_y b}{\Delta_x b}\right) \tag{11}$$

According to its gradient's angle, each block$b_i$is related with a pattern group. Best counterpart pattern for the block is then selected from the group. To this, each block is subtracted first by its mean value:

$$a_i = b_i - mean(b_i) \times \begin{pmatrix} 1 & 1 & 1 \\ 1 & 1 & 1 \\ 1 & 1 & 1 \end{pmatrix} \tag{12}$$

Then$a_i$undergoes a sign function.

$$a_i^s = sign(a_i) \tag{13}$$

Finally, $a_i^s$is multiplied element wise (element wise production is showed as.$\times$) by all patterns in group and the elements of resultant matrix are summed.

$$\hat{a}_{ik} = sum(a_i^s .\times vp_k) \tag{14}$$

The highest value of$\hat{a}_{ik}$corresponds to the most appropriate visual pattern$vp_k$for blockb_i.

Since choosing a small size for blocks provides weak denoising in homogenous parts of image [9], a block of size 3×3 is not a good candidate for NLM. To overcome this drawback, a larger odd size (e.g.$5 \times 5, 7 \times 7$)must be used.

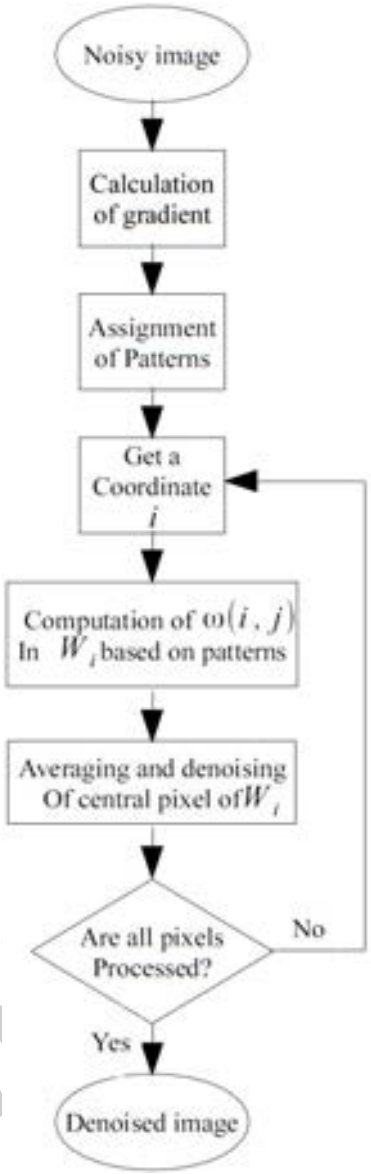

Figure 3. Flowchart of proposed method

In this paper the denoising is done for a set of pixels instead of an alone pixel in each weighted averaging. To this , Eq. 2 is modified as:

$$\hat{p}_i = \sum_{j \in W_i} \frac{\omega(i,j) p_j}{\sum_{j \in W_i} \omega(i,j)} \quad (15)$$

Where p_j present blocks centered on pixel$j$ and$\hat{p}_i$is the result of averaging on them. To determine a proper block sizefor p_j, experiments with different size of blocks $(1 \times 1, 3 \times 3, 5 \times 5and7 \times 7)$over several images are performed. As table 6 suggests the difference between one by one denoising of pixels and denoising them in a block wisemanner with block size of$3 \times 3$is negligible; however, denoising of several pixels with one averaging is by so far faster than original method.

According to the obtained results, denoising2×2blocks by one weighted averaging is chosen. The proposed method is as follows.

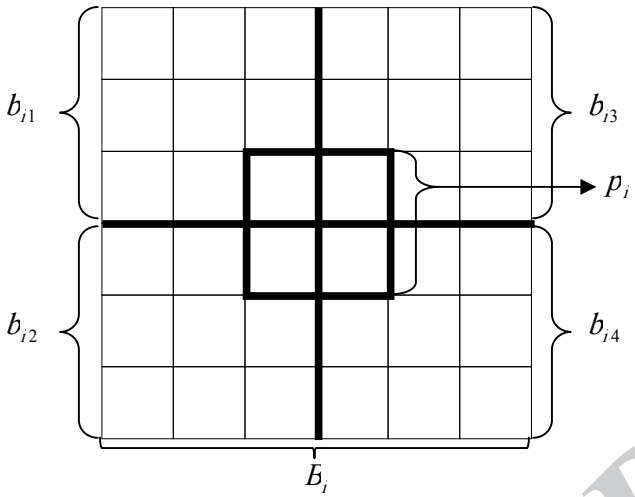

Figure 4.Dividing a block in to 4 blocks

After decomposing the noisy image into3×3blocks, each blockB_i is divided to four sub-blocks,b_{ik}(Figure 4).

Letvp_{ik} are visual patterns related tob_{ik}in the central blockofW_i. The component of blocksb_{ik}andb_{jk}in space with unit vectors$vp_{ik}$are computed:

$$C_{ik} = sum(vp_{ik} \times a_{ik}) \tag{16}$$

$$C_{jk} = sum(vp_{ik} \times a_{jk}) \tag{17}$$

The summation of these blocks is computed as another comparable measure.

$$S_{ik} = sum(b_{ik}) \tag{18}$$

$$S_{jk} = sum(b_{jk}) \tag{19}$$

The distance between blocks$B_i$and$B_j$is computed

$$d_{ij}^2 = \sum_{k=1}^{4} \left((C_{ik} - C_{jk})^2 + (S_{ik} - S_{jk})^2 \right) \tag{20}$$

Weights for blocks$p_j$are computed:

$$\omega(i,j) = e^{-\frac{d_{ij}^2}{h^2}} \tag{21}$$

And finally the denoised block is obtained by averaging:

$$\hat{p}_i = \sum_{j \in W_i} \frac{\omega(i,j) p_j}{\sum_{j \in W_i} \omega(i,j)} \tag{22}$$

It is to be noted that the computational complexity of the original NLM is of order$\mathcal{O}(B \times N \times S)$where$N$is number of pixels in image and$S$is number of pixels in neighborhoodW_i, and for Tasdizen's method it is of order$\mathcal{O}(r \times N \times S)$where$r$is number of dimensions after dimension reduction.The proposed method denoises image in a space of 8 dimensions (4 visual patterns and 4 summations of blocks). Thus computational complexity of proposed method is of order$\mathcal{O}(N \times S)$. Note that, in only one averaging, the proposedmethod denoises 4 pixels instead of one, and it makes it about 4 times faster.

6. Experimental Results

To evaluate the performance of the proposed method, a comparative study with some other modern methods is presented. The experiments are applied on5 images of different scales, sizes and contents, all of 256 gray levels. For the proposed method, the search area size$S$is set to$21 \times 21$and filtering parameter$h$is tuned to maximize PSNR. For the ordinary NLM method, blocks$b_i$are considered to be of size7×7. The state-of-the-art methods compared here are NLM-C_p [24], NLM-SAP [15] and NLM-PCA [11] in addition to original method NLM [6]. All the simulations are done using MATLAB R2012a, on a Vaio PCCW2DGX laptop.

To evaluate these methods, six IQA criteria are used to compare these methods.

PSNR: As a classic image quality assessment criterion, it is derived as follows.

$$PSNR = 10log_{10}\frac{R^2}{MSE} \quad (23)$$

Where$R$is maximum gray level value of image.

FOM: Figure of merit uses the distances between edge pixels in the filtered and original images to build a reliable criterion [19].

$$FOM = \frac{1}{I_N}\sum_{i=1}^{I_A}\frac{1}{1+ad^2} \quad (24)$$

Where$I_N = max(I_I, I_A)$, and$I_I$and$I_A$represent the number of edge map points in original and filtered images, respectively.$a$is a scaling constant (1/9), and$d$is the separation distance of two edge points in original and filtered images.

Two mentioned criteria are based on mathematical philosophy; however, the proposed method is adapted for being favorable to HVS. Thus some measures taking HVS into account are used:

MSSIM: Under the assumption that human visual perception is highly adapted for extracting structural information from a scene, MSSIM provides an alternative framework for quality assessment based on the degradation of structural information. MSSIM is ranged from 0 to one, and a bigger value for MSSIM means a higher quality of the denoised image [20].

NSER: Rapid change in light intensity has a considerable effect on human sight in different scales. It can be modeled by a series of LOG filters. NSER is based on edge detection by LOG filter with different scales, and locating zero crosses for original and denoised image, then counting the edge points that are in same places in both edge maps. In other words, the more correlation between edge maps exists, the more NSER value is obtained [21].

PSNR-HVS-M: In one hand, contrast sensitivity function (CSF) shows, how much detectable is the change in any DCT coefficient of a block in image, by HVS. On the other hand, the effect of DCT coefficients of a block of image on the sensitivity to change of each other is called between-coefficient contrast masking. Taking these two properties of HVS into account, authors of [22] proposed the measure PSNR-HVS-M for IQA.

Method noise: Method noise is defined as the difference between noisy and denoised image [13].

$$MN(i) = v(i) - \hat{u}(i) \quad (25)$$

The less image details perceivable in method noise image, the better detail preserving ability of denoising method, and also better noise reduction of denoising process is obtained as more noise in method noise image. In other words, similarity between method noise and white Gaussian noise shows the superiority of denoising method. For better visibility of details, method noise image is added to 127.

In tables 1-5 three best results are shadowed as golden silver and bronze colors, respectively. As table 1 suggests, although performance of proposed method is not considerable from a mathematical IQA measure like PSNR point of view, however, these kind of measures are not related to HVS.

According to [23], MSSIM and PSNR-HVS-M are good criteria for different kind of distortions and especially the latter one has a remarkable accordance to HVS on noise distortion. In tables 2 and 3 image quality of the results of proposed method is confirmed by these two criteria, and on average the method has the best performance in comparison to other compared methods. The superiority of the proposed method is also visible in tables 4 and 5 by NSER and FOM.

The results of image denoising by the proposed method as well as some state-of-the-art methods are presented in figure 5. As this figure confirms, details are well preserved by the proposed method. This could be seen in the scarf of Barbara, Lena's hat and fur of mandrill. These remarks are visible in the method noises depicted in Figure 6. It is to be noted that the additionally artifacts seen in the results of method NLM-PCA, are not visible in VPID. To achieve a better comparison on denoised images, the results are compared in tables 1-5.

Table 1. Comparison of proposed method VPID with NLM [6], NLM-C_p [24], NLM-SAP [15] and NLM-PCA [11], based on PSNR (dB).

Image	σ_n	NLM	NLM-C_p	NLM-SAP	NLM-PCA	VPID
Lena	10	34.11	35.10	35.07	34.45	34.81
	20	31.03	31.74	31.97	31.94	31.95
	40	27.84	28.26	28.29	29.28	28.75
Barbara	10	33.07	34.02	33.76	32.56	32.39
	20	29.50	30.16	30.31	29.63	29.02
	40	25.81	26.07	25.93	26.76	25.60
Mandrill	10	29.29	29.90	29.56	29.22	29.60
	20	25.16	25.67	25.73	25.54	25.60
	40	22.17	22.58	22.07	22.53	22.60
Camera man	10	32.53	33.60	33.55	31.60	32.73
	20	28.69	29.92	29.76	29.07	29.37
	40	25.58	26.45	26.24	26.42	26.36
House	10	34.67	35.69	35.52	34.82	35.18
	20	31.74	32.45	32.62	32.47	32.62
	40	27.66	28.39	27.98	29.49	28.98
Average		29.26	30.00	29.89	29.72	29.70

Table 2. Comparison of proposed method VPID with NLM [6], NLM-C_p [24], NLM-SAP [15] and NLM-PCA [11], based on MSSIM×10^4.

Image	σ_n	NLM	NLM-C_p	NLM-SAP	NLM-PCA	VPID
Lena	10	9723	9787	9781	9765	9782
	20	9460	9560	9550	9595	9579
	40	8993	9118	9056	9231	9141
Barbara	10	9795	9837	9838	9782	9831
	20	9541	9620	9610	9591	9618
	40	9055	9121	9049	9199	9102
Mandrill	10	9704	9738	9736	9653	9761
	20	9021	9257	9231	9237	9391
	40	7957	8279	7968	8292	8552
Camera man	10	9808	9826	9829	9724	9828
	20	9474	9621	9563	9573	9596
	40	9127	9220	9108	9233	9190
House	10	9722	9788	9766	9749	9767
	20	9596	9617	9605	9648	9641
	40	9197	9237	9146	9348	9284
Average		9345	9442	9389	9441	9471

Table 3. Comparison of proposed method VPID with NLM [6], NLM-C_p [24], NLM-SAP [15] and NLM-PCA [11], based on PSNR-HVS-M (dB).

Image	σ_n	NLM	NLM-C_p	NLM-SAP	NLM-PCA	VPID
Lena	10	33.58	34.65	34.83	34.74	34.98
	20	28.49	29.68	29.55	30.33	30.19
	40	24.17	25.25	24.37	26.03	25.51
Barbara	10	33.80	34.85	35.09	33.76	35.16
	20	28.49	29.48	29.32	29.39	29.90
	40	24.11	24.57	23.82	25.10	24.88
Mandrill	10	32.57	32.77	33.05	31.92	33.39
	20	25.29	26.02	26.20	26.44	26.98
	40	20.64	21.24	20.32	21.53	22.01
Camera man	10	35.22	35.49	35.50	33.38	35.81
	20	28.57	29.99	29.43	29.85	30.14
	40	24.30	25.17	24.42	25.66	25.48
House	10	34.47	35.71	35.53	35.42	35.62
	20	30.50	31.10	30.97	31.85	31.70
	40	25.09	25.73	24.36	26.95	26.45
Average		28.62	29.45	29.12	29.80	29.88

Table 4. Comparison of proposed method VPID with NLM [6], NLM-C_p [24], NLM-SAP [15] and NLM-PCA [11], based on NSER.

Image	σ_n	NLM	NLM-C_p	NLM-SAP	NLM-PCA	VPID
Lena	10	2.404	2.641	2.637	2.612	2.667
	20	1.658	1.873	1.835	1.907	1.970
	40	1.195	1.304	1.236	1.348	1.359
Barbara	10	2.743	2.918	2.961	2.798	3.098
	20	1.924	2.111	2.088	2.117	2.267
	40	1.398	1.455	1.342	1.504	1.519
Mandrill	10	3.092	3.016	3.132	2.866	3.197
	20	1.803	1.942	1.960	1.920	2.100
	40	1.160	1.251	1.162	1.215	1.328
Camera man	10	3.106	3.082	3.046	2.884	3.176
	20	1.991	2.214	2.196	2.178	2.319
	40	1.496	1.577	1.540	1.624	1.664
House	10	2.716	2.878	2.965	2.740	2.923
	20	2.096	2.173	2.145	2.221	2.262
	40	1.451	1.450	1.333	1.598	1.638
Average		2.016	2.126	2.105	2.102	2.232

Table 5. Comparison of proposed method VPID with NLM [6], NLM-C_p [24], NLM-SAP [15] and NLM-PCA [11], based on FOM×10^4.

Image	σ_n	NLM	NLM-C_p	NLM-SAP	NLM-PCA	VPID
Lena	10	5808	6149	6232	6096	6219
	20	3919	4481	4300	4633	4549
	40	2524	3150	2499	3275	3094
Barbara	10	6509	6742	6807	6258	6770
	20	4435	5010	4720	4820	5225
	40	3201	3460	2951	3447	3489
Mandrill	10	6732	6675	6778	6462	6924
	20	4560	5078	4788	4912	5281
	40	3084	3544	2604	3376	3743
Camera man	10	6729	6548	6890	5888	7114
	20	4548	4930	4971	4982	5155
	40	3644	3816	3671	3903	3835
House	10	7624	7854	7902	7864	7958
	20	6409	6564	6575	6770	6629
	40	4751	5029	4577	5198	4932
Average		4965	5269	5084	5192	5394

In brief, it could be concluded that however the-state-of-the-art image denoising methods provide high quality results in a mathematical criteria point of view, none of them have taken human visual systems properties into account. Hence, they achieve a lower performance than the proposed method according to HVS based criteria.

Table 6. Comparison of original method NLM with examination of denoising of several pixels simultaneously, based on PSNR (dB).

Image	σ_n	NLM	Denoising of several pixels		
			3×3	5×5	7×7
Lena	10	34.11	34.08	33.95	33.62
	20	31.03	30.96	30.80	30.40
	40	27.84	27.73	27.52	27.12
Barbara	10	33.07	32.97	32.82	32.46
	20	29.50	29.39	29.20	28.80
	40	25.81	25.71	25.53	25.24
Mandrill	10	29.29	29.28	29.26	29.19
	20	25.16	25.13	25.08	24.96
	40	22.17	22.13	22.08	21.97
Camera man	10	32.53	32.51	32.46	32.36
	20	28.69	28.64	28.50	28.15
	40	25.58	25.42	25.23	24.78
House	10	34.67	34.58	34.43	34.15
	20	31.74	31.51	31.31	30.82
	40	27.66	27.59	27.41	26.92
Average		29.26	29.18	29.04	28.73

Figure 5. From left to right: Original image, result of denoising of noisy images with noise standard deviation 20 by NLM [6], NLM-C_p [24], NLM-SAP [15], NLM-PCA [11] and Proposed method (VPID). From top to bottom: Barbara, Cameraman and Lena images.

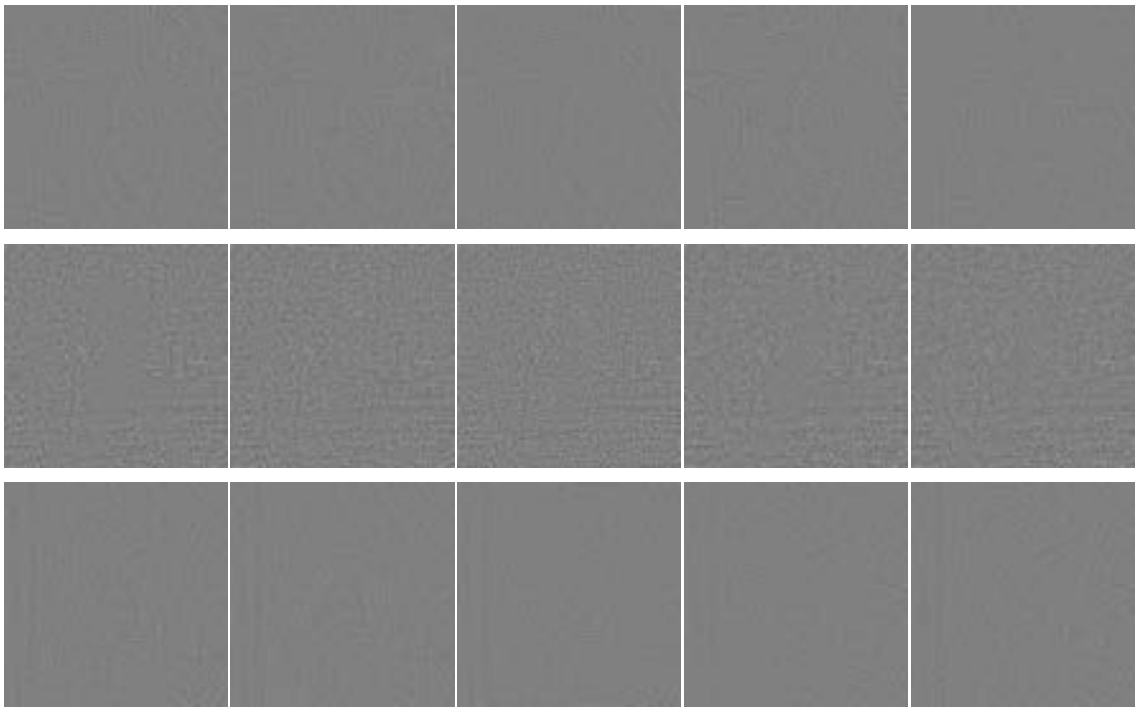

Figure 6. From left to right: method noise of denoised noisy images with noise standard deviation 20 by NLM [6], NLM-Cp [24], NLM-SAP [15], NLM-PCA [11] and Proposed method (VPID). From top to bottom: Barbara, Cameraman and Lena images.

7. Conclusion

In this paper, a new image denoising method based on visual patterns was proposed. The proposed method takes human visual system's properties into account to achieve more favorable results according to human eyes. This was done by using some adapted patterns in sole of non-local means method. To evaluate the performance of the proposed method, a comparative experiment with some state-of-the-art denoising methods was performed. Several HVS based criteria were used to compare the results. The obtained results confirmed the superiority of the proposed method from an HVS point of view.

8. References

[1] S.M. Smith and J.M. Brady, "SUSAN-A new approach to low level image processing," *Int'l J. Comput. Vis.*, vol. 23, no. 1, pp. 45–78, 1997.

[2] C. Tomasi and R. Manduchi, "Bilateral filtering for gray and color images," *in Proc. 6th IEEE Inter. Conf. Comput. Vis., (ICCV), Bombay, India*, pp. 839-846, 1998.

[3] P. Perona and J. Malik, "Scale-space and edge detection using anisotropic diffusion," *IEEE Trans. Pattern Anal. Mach. Intell.*, vol. 12, no. 7, pp. 629–639, 1990.

[4] L.I. Rudin, S. Osher, E. Fatemi, "Nonlinear total variation based noise removal algorithms," *Physica D,* vol. 60, pp. 259-268, 1992.

[5] R.R. Coifman and D.L. Donoho, "Translation-invariant denoising," *in Waveletes and Statistics, A. Antoniadis and G. Oppenheim, Eds. New York: Springer-Verlag*, pp. 125–150, 1995.

[6] A. Buades, B. Coll, and J.M. Morel, "A non-local algorithm for image denoising," *in Proc. IEEE Comput. Soc. Conf. Comput. Vis. Pattern Recogn., (CVPR)*, vol. 2, pp. 60-65, 2005.

[7] M. Mahmoudi and G. Sapiro, "Fast image and video denoising via non-local means of similar neighborhoods," *IEEE Signal Process. Lett.*, vol. 12, no. 12, pp. 839–842, 2005.
[8] A.A. Tahmouresi, S. Saryazdi, S.R. Seydnejad, "An efficient hybrid non-local means and Gaussian image denoising," *in proc. IEEE Inter. Conf. Comput. and Info. Science, (CICIS), Zanjan, Iran,* pp. 241-244, 2011.
[9] V. Duval, J.F. Aujol, and Y. Gousseau, "On the parameter choice for the non-local means," *Tech. Rep.* HAL-00468856, HAL, 2010.
[10] J. Orchard, M. Ebrahimi, and A. Wong, "Efficient non-local means denoising using the SVD," *in Proc. 15th IEEE* Inter. *Conf. Image Process. (ICIP), San Diego, CA*, pp. 1732-1735, 2008.
[11] T. Tasdizen, "Principal neighborhood dictionaries for non-local means image denoising," *IEEE Trans. Image Process.* vol. 18, pp. 2649-2660, 2009.
[12] R.C. Gonzalez, R.E. Woods, "Digital image processing," *Second ed., Pearson Prentice Hall*, 2002.
[13] A. Buades, B. Coll, and J.M. Morel, "A review of image denoising algorithms, with a new one," *Multiscale Model. Simul. (SIAM Interdisciplin.),* vol. 4, no. 2, pp. 490–530, 2005.
[14] A. Buades, B. Coll, and J.M. Morel, "Self-similarity-based image denoising," *Commun. ACM,* vol. 54, no. 5, pp. 109–117, 2011.
[15] C.A. Deledalle, V. Duval, J. Salmon, "Non-local Methods with Shape-Adaptive Patches (NLM-SAP)," *Jour. of Math. imag. and vis.* pp. 1-18, 2011.
[16] D. Van de ville and M. Kocher, "Sure Based Non-Local Means," *IEEE Signal Process. Lett.*, vol. 16, no. 11, pp. 973–976, 2009.
[17] D. Chen and A.C. Bovik, "Visual pattern coding," *IEEE Trans. Commun.*, vol. COM-38, pp. 2137-2146, 1990.
[18] E. B. Goldstein, Sensation and Perception, *Cengage Learning*, 2010.
[19] W.K. Pratt, "Digital Image Processing," *Third ed., New York: Wiley,* 2001.
[20] Z. Wang, A.C. Bovik, H.R. Sheikh, and E.P. Simoncelli, "Image quality assessment: from error visibility to structural similarity," *IEEE Trans. Signal Proc.*, vol 13, no. 4, pp 600-612, 2004.
[21] M. Zhang, X. Mou and L. Zhang, "Non-shift edge based ratio (NSER): an image quality assessment metric based on early vision features," *IEEE Signal Process. Lett.*, vol. 18, no. 5, pp. 315–318, 2011.
[22] N. Ponomarenko, F. Silvestri, K. Egiazarian, Carli M., Astola J., Lukin V. "On between-oefficient contrast masking of DCT basis functions", *in Proc. Third Int. Workshop Video Process. and Quality Metrics, USA,* - 4 p, 2007.
[23] N. Ponomarenko, V. Lukin, A. Zelensky, K. Egiazarian, M. Carli, and F. Battisti, "Tid2008 - a database for evaluation of full reference visual quality assessment metrics," *Advances of Modern Radioelectronics,* vol. 10, pp. 30–45, 2009. http://www.ponomarenko.in-fo/tid2008.htm.
[24] V. Dore and M. Cheriet, "Robust NL-Means Filter With Optimal Pixel-Wise Smoothing Parameter for Statistical Image Denoising" *IEEE Trans. Signal Process.* , vol. 57, no. 5, pp. 1703–1716, 2009.